

Closed-loop identification of the time-varying dynamics of variable-speed wind turbines

J. W. van Wingerden^{*,†}, I. Houtzager, F. Felici and M. Verhaegen

*Delft Center for Systems and Control, Delft University of Technology, Mekelweg 2,
2628 CD Delft, The Netherlands*

SUMMARY

The trend with offshore wind turbines is to increase the rotor diameter as much as possible to decrease the costs per kWh. The increasing dimensions have led to the relative increase in the loads on the wind turbine structure. Because of the increasing rotor size and the spatial load variations along the blade, it is necessary to react to turbulence in a more detailed way: each blade separately and at several separate radial distances. This combined with the strong nonlinear behavior of wind turbines motivates the need for accurate linear parameter-varying (LPV) models for which advanced control synthesis techniques exist within the robust control framework. In this paper we present a closed-loop LPV identification algorithm that uses dedicated scheduling sequences to identify the rotational dynamics of a wind turbine. We assume that the system undergoes the same time variation several times, which makes it possible to use time-invariant identification methods as the input and the output data are chosen from the same point in the variation of the system. We use time-invariant techniques to identify a number of extended observability matrices and state sequences that are inherent to subspace identification identified in a different state basis. We show that by formulating an intersection problem all states can be reconstructed in a general state basis from which the system matrices can be estimated. The novel algorithm is applied on a wind turbine model operating in closed loop. Copyright © 2008 John Wiley & Sons, Ltd.

Received 30 July 2007; Revised 14 January 2008; Accepted 4 March 2008

KEY WORDS: LPV; wind turbine; subspace identification; individual pitch control

*Correspondence to: J. W. van Wingerden, Delft Center for Systems and Control, Delft University of Technology, Mekelweg 2, 2628 CD Delft, The Netherlands.

†E-mail: J.W.vanWingerden@tudelft.nl

Contract/grant sponsor: Technology Foundation STW
Contract/grant sponsor: NWO
Contract/grant sponsor: Ministry of Economic Affairs

1. INTRODUCTION

The trend with offshore wind turbines is to increase the rotor diameter as much as possible. The reason is that the foundation costs of offshore wind turbines amount to a large part of the total costs. Therefore, designers want to increase the energy yield per wind turbine, which increases with the square of the rotor diameter, as much as possible to reduce the costs. Hence, modern wind turbines designed for offshore application have become the largest rotating machines on earth, with the length of one blade almost equal to the entire span of a Boeing 747. The increasing dimensions have led to the relative increase in the loads on the wind turbine structure.

There have been two main control concepts to keep the loads within acceptable limits. The concept used from the seventies until the nineties in the previous century was the ‘Danish concept’ [1]. The turbines making use of this concept combine constant rotor speed with stall of the flow around the rotor blades and are stable by design: increasing wind speeds automatically induce increasing drag forces that limit the absorbed power. In that period, all other control options were considered too complex. However, most modern large wind turbines run at variable rotational speed, combined with the adjustment of the collective pitch angle of the blades to optimize energy yield and to control the loads [2]. This is a step forward: the control of the blade pitch angle has not only led to power regulation but also to a significantly lighter blade construction due to the lower load spectrum and a lighter gear box due to shaved torque peaks. However, full-span collective pitch control can only handle slow wind changes that affect the entire rotor. Because of the increasing rotor size, it is necessary to react on turbulence in a more detailed way: each blade separately and at several separate radial distances. This first item is dealt with in individual pitch control (IPC), motivated by the helicopter industry [3–6], which is the latest development in the wind turbine industry to further minimize the loads. With this latest control concept, each blade is pitched individually to suppress the harmonic loads. The controllers are designed using linear controller synthesis and are gain scheduled afterwards to compensate for the nonlinear behavior of the variable-speed wind turbines. However, this method does not guarantee any stability or performance [7]. In recent work [8–10], the linear parameter-varying (LPV) framework is proposed for the design of feedback controllers in the wind energy. These LPV systems can be seen as a particular type of time-varying system, where the variation depends explicitly on a time-varying parameter referred to as the scheduling or weight sequence. For wind turbines, this is typically the rotor speed, rotor position, and pitch position. The main advantage of the LPV controller synthesis problem is that it results in robust gain-scheduled controllers that have the property to have guaranteed performance and stability over the complete operation envelop.

For LPV control, it is important to have an accurate mathematical model of the system under consideration because the synthesis problem requires a model. Common practice in the wind industry is to model the dynamics using first principles [11]. However, this approach has a number of disadvantages: time consuming, over/under modeling, uncertainties, and complexity. However, efficient methods to obtain mathematical models from measurement data exist; these methods are referred to as system identification. Using the available measurements only the most important dynamics is modeled. This implies that system identification gives a compact-sized model that is suitable for controller (re)design, load calculations, and model validation. Linear time-invariant (LTI) system identification is well established and few applications can be reported in the wind energy community [12–15]. However, wind turbines are nonlinear systems and as stated before they can be reformulated in the LPV framework.

An overview of past literature in LPV identification setting can be found in [16]. It is possible to distinguish between identification techniques for different types of scheduling sequences. For the case where this sequence can be arbitrarily varying, the identification problem has proven to be challenging. The subspace identification method proposed in [17] and later improved in [18] has the inherent drawback that it requires an approximation, neglecting certain terms and possibly leading to biased results. This method can, however, be used as an initial estimate for a parametric identification method as proposed in [19]. Because of these difficulties, it is interesting to investigate whether the use of dedicated scheduling sequences facilitates the identification of LPV systems. Specific cases of scheduling sequences have been studied, such as the case of abrupt switching, which leads to piecewise affine (hybrid) systems [20], and periodic scheduling [21].

In this paper we tackle a part of the LPV system identification problem for wind turbines. We will consider the rotational dynamics of the wind turbine where the scheduling sequence undergoes the same time variation several times, which makes it possible to use a number of well-established steps from LTI system identification. Furthermore, the focus of this paper will be on state-space LPV systems operating in closed loop for which the scheduling sequence repeats itself a number of times (ensemble identification). State-space LPV systems are considered in particular instead of their input/output counterparts because of their ability to efficiently handle multiple inputs and outputs, which is essential for wind turbines. Therefore, the identification of LPV state-space models is of interest. The work we present is strongly related to [21] where an open-loop LPV system identification scheme with a periodic scheduling sequence is used, which significantly simplifies the LPV system identification problem. However, the MOESP type of algorithm used in this particular paper gives biased results for systems operating under closed-loop conditions. The first main contribution of this paper is that we use ideas from closed-loop system identification [22–24], where no assumption is made with respect to the correlation between the input and the noise sequence. The second contribution is that we can deal with ensemble data (no perfect periodic scheduling signal is required). The third contribution is the application on a challenging wind turbine model. The first contributions are essential for wind turbines because wind turbines are unstable systems and consequently have to operate in closed loop, and the rotational dynamics of a variable-speed wind turbine are not exactly periodic but still it undergoes the same time variation a number of times.

The remainder of this paper is organized as follows: In Section 2, the theoretic framework is presented for the identification of closed-loop LPV systems using a dedicated scheduling sequence. In Section 3, the algorithm is applied to an LPV model of a wind turbine. In the final sections we present the challenges left in the field of the identification of wind turbines and we present the conclusions of this paper.

2. LPV IDENTIFICATION FOR DEDICATED SCHEDULING SEQUENCES

For linear time-varying (LTV) systems, it is well known that ensemble identification can be used to obtain accurate models of the LTV system. However, when the time variation is changing these models are not valid anymore. In this section an algorithm is presented that uses ensemble identification to construct an LPV model. First, we describe a general problem formulation and the assumptions are given. Then a number of extended observability matrices are estimated assuming that the same time-varying behavior is present a number of times. These observability matrices have the inherent drawback that they are identified in a different state basis. This can be solved

by solving an intersection problem. When the similarity transformations are known, the states can be transformed into the same global state basis and the system matrices can be reconstructed by solving a set of linear equations.

2.1. Problem formulation

Consider the LPV system

$$x_{k+1} = A_k x_k + B_k u_k + K e_k \quad (1)$$

$$y_k = C_k x_k + D_k u_k + e_k \quad (2)$$

where $x_k \in \mathbb{R}^n$, $u_k \in \mathbb{R}^r$, and $y_k \in \mathbb{R}^\ell$, are the state, input, and output vectors, and the noise sequence $e_k \in \mathbb{R}^\ell$ is a zero-mean white-noise sequence.

The time-varying system matrices are given by

$$A_k = \sum_{i=1}^m A^{(i)} \mu_k^{(i)} \quad (3)$$

where m represents the number of LPV system matrices. In an identical manner, the matrices B_k , C_k , and D_k are defined. In these expressions, $A^{(i)} \in \mathbb{R}^{n \times n}$, $B^{(i)} \in \mathbb{R}^{n \times r}$, $C^{(i)} \in \mathbb{R}^{\ell \times n}$, $D^{(i)} \in \mathbb{R}^{\ell \times r}$, and $K \in \mathbb{R}^{n \times \ell}$ are referred to as the system matrices. The model weights are $\mu_k^{(i)} \in \mathbb{R}$. Note that the system matrices depend in a linear manner on the time-varying scheduling vector

$$\mu_k = (\mu_k^{(1)} \quad \mu_k^{(2)} \quad \cdots \quad \mu_k^{(m)})^T \quad (4)$$

To include the case of affine dependence, one can set the first entry of the scheduling vector to unity: $\mu_k^{(1)} = 1$, $\forall k$. It is required that the terms of the scheduling sequence are linearly independent, such that

$$\text{rank}([\mu_0 \quad \mu_1 \quad \cdots \quad \mu_{s-1}]) = m \quad (5)$$

and $s \geq m$.

The state-space realization given in (1)–(2) can be expressed in the predictor form as follows

$$x_{k+1} = \tilde{A}_k x_k + \tilde{B}_k u_k + K y_k \quad (6)$$

$$y_k = C_k x_k + D_k u_k + e_k \quad (7)$$

where $\tilde{A}_k = A_k - K C_k$ and $\tilde{B}_k = B_k - K D_k$.[‡] It is well known that an invertible linear transformation of the state does not change the input–output behavior of a state-space system. Therefore, we can only determine the system matrices up to a similarity transformation $T \in \mathbb{R}^{n \times n}$: $T^{-1} A^{(i)} T$, $T^{-1} B^{(i)}$, $T^{-1} K$, $C^{(i)} T$, and $D^{(i)}$.

The identification problem can now be formulated as follows: given the input sequence u_k , the output sequence y_k , and the scheduling sequence μ_k to find all the LPV system matrices $A^{(i)}$, $B^{(i)}$, $C^{(i)}$, $D^{(i)}$, and K up to a global similarity transformation.

[‡]Observe that the matrix K is time invariant. This is done to make the notation and derivation not too complex.

2.2. Definitions and assumptions

We define the stacked output vector \bar{y}_k^i as

$$\bar{y}_k^i = (y_k^T \ y_{k+1}^T \ \cdots \ y_{k+i-1}^T)^T \quad (8)$$

and similarly the stacked input \bar{u}_k^i , stacked noise \bar{e}_k^i , and stacked scheduling $\bar{\mu}_k^i$ are defined. In parallel to what is done in LTI identification for time-varying systems also an observability matrix can be derived

$$\tilde{\mathcal{O}}_k^f = \begin{pmatrix} C_k \\ C_{k+1}\tilde{A}_k \\ C_{k+2}\tilde{A}_{k+1}\tilde{A}_k \\ \vdots \\ C_{k+f-1}\tilde{A}_{k+f-2}\cdots\tilde{A}_k \end{pmatrix} \in \mathbb{R}^{\ell f \times n} \quad (9)$$

where $\tilde{\mathcal{O}}_k^f$ is the time-varying extended observability matrix at time instance k , and f is referred to as the future window size. In what follows, it is assumed that $\tilde{\mathcal{O}}_k^f$ has full column rank for all k 's, which is equivalent to requiring that the system is observable on all intervals of length f according to the condition for observability of LPV systems in [25].

We also define the matrices

$$\tilde{\Phi}_k^f = \begin{pmatrix} D_k & 0 & \cdots & 0 \\ C_{k+1}\tilde{B}_k & D_{k+1} & & \\ C_{k+2}\tilde{A}_{k+1}\tilde{B}_k & C_{k+2}\tilde{B}_{k+1} & & \\ \vdots & \vdots & \ddots & \\ C_{k+f-1}\tilde{A}_{k+f-2}\cdots\tilde{A}_{k+1}\tilde{B}_k & C_{k+f-1}\tilde{A}_{k+f-2}\cdots\tilde{A}_{k+2}\tilde{B}_{k+1} & & D_{k+f-1} \end{pmatrix} \in \mathbb{R}^{\ell f \times r f} \quad (10)$$

$$\tilde{\Psi}_k^f = \begin{pmatrix} 0 & 0 & \cdots & 0 \\ C_{k+1}K & 0 & & \\ C_{k+2}\tilde{A}_{k+1}K & C_{k+2}K & & \\ \vdots & \vdots & \ddots & \\ C_{k+f-1}\tilde{A}_{k+f-2}\cdots\tilde{A}_{k+1}K & C_{k+f-1}\tilde{A}_{k+f-2}\cdots\tilde{A}_{k+2}K & & 0 \end{pmatrix} \in \mathbb{R}^{\ell f \times \ell f} \quad (11)$$

With the previous definitions it holds that for all $k = \{0, \dots, N-1\}$

$$\bar{y}_k^f = \tilde{\mathcal{O}}_k^f x_k + \tilde{\Phi}_k^f \bar{u}_k^f + \tilde{\Psi}_k^f \bar{y}_k^f + \bar{e}_k^f \quad (12)$$

This data equation is the starting point for many subspace identification schemes. However, now the matrices \tilde{C}_k^f , $\tilde{\Phi}_k^f$, and $\tilde{\Psi}_k^f$ are time varying.

2.3. Step 1: ensemble identification

In this section we assume that the scheduling sequence, which determines the time-varying behavior of the system repeats itself a number of times or with other words: the system undergoes the same time variation a number of times. The length of this repeating scheduling sequence is at least $p+f$ samples long, where f is referred to as the future window (see the previous section) and in a similar way p is referred to as the past window. The indices where such a scheduling sequence starts are defined as

$$\tilde{t}_j = [t_{j,1}, \dots, t_{j,\alpha^j}]$$

where $t_{j,i} \in \mathbb{N}$ is the starting point of the interval and the number of intervals equals α^j . \tilde{t}_j with $j \in \{1, 2, \dots, v\}$ are intervals where the scheduling sequence j is active and $v \in \mathbb{N}$ represents the number of different scheduling sequences. This definition is illustrated in Figure 1. A special signal that satisfies this definition is a period scheduling [21, 26]. In this case the white areas in Figure 1 are removed such that we have a perfect periodic signal left. In [21] the scheduling sequence should be perfectly periodic during the identification experiment to identify an LPV model, although afterwards this identified model is also valid for every random scheduling sequence. The rotational dynamics of variable-speed wind turbines is not perfectly periodic, although it undergoes the same time variation a number of times. Also for other processes such as the behavior of a wafer stage or a rotating device, the same dynamics will occur a number of times (ensembles). The periodic scheduling signal can be seen as a subset of the definition given above. In this paper we show how we can extend the periodic result to ensemble data.

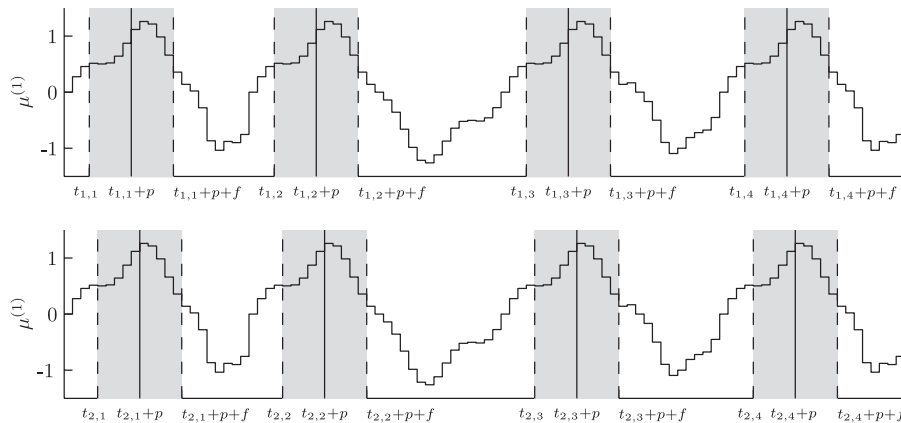


Figure 1. Illustrative example of a possible scheduling sequence. In the top figure, the gray shaded areas are of length $p+f$ and illustrate the areas where the same scheduling segment is active. The starting points of the intervals are defined by \tilde{t}_1 . In the bottom figure, the same scheduling sequence is given. However, a different scheduling segment is depicted by the gray areas. The areas start one sample later and the starting points are defined by \tilde{t}_2 .

When we evaluate (12) for all $k \in \tilde{t}_j + p$,[§] the observability matrices $\tilde{\Phi}_k^f$ and $\tilde{\Psi}_k^f$ become time invariant on that particular set. We define these matrices as follows

$$\tilde{\mathcal{O}}_j^f = \tilde{\mathcal{O}}_k^f \quad \forall k \in \tilde{t}_j + p \quad (13)$$

$$\tilde{\mu}_j^{p+f} = \tilde{\mu}_k^{p+f} \quad \forall k \in \tilde{t}_j \quad (14)$$

and in a similar way this can be done for $\tilde{\Phi}_k^f$ and $\tilde{\Psi}_k^f$.

The state can be expressed in the known past inputs \bar{u}_k^p , outputs \bar{y}_k^p , and the initial state. This state x_{k+p} is given by

$$x_{k+p} = (\tilde{A}_{k+p} \tilde{A}_{k+p-1} \dots \tilde{A}_k) x_k + (\tilde{\mathcal{C}}_k^p \quad \tilde{\mathcal{H}}_k^p) \begin{pmatrix} \bar{u}_k^p \\ \bar{y}_k^p \end{pmatrix} \quad (15)$$

where $\tilde{\mathcal{C}}_k^p$ is the time-varying controllability matrix, which is defined as

$$\tilde{\mathcal{C}}_k^p = (\tilde{A}_{k+p-1} \dots \tilde{A}_{k+1} \tilde{B}_k \quad \dots \quad \tilde{A}_{k+p-1} \tilde{B}_{k+p-2} \quad \tilde{B}_{k+p-1}) \quad (16)$$

and

$$\tilde{\mathcal{H}}_k^p = (\tilde{A}_{k+p-1} \dots \tilde{A}_{k+1} K \quad \dots \quad \tilde{A}_{k+p-1} K \quad K) \quad (17)$$

We assume that the LPV system given in (6)–(7) is LPV stable [7].[¶] By choosing p large enough, the contribution of the initial state to the state x_{k+p} can be made arbitrarily small. In a number of LTI subspace methods, it is well known to disregard the effect of the initial state resulting in a biased estimate, although this bias can be made arbitrarily small by choosing p larger [23, 27]. The first step in the closed-loop system identification scheme is to use this approximation to get an estimate of $\tilde{\Phi}_k^f$ and $\tilde{\Psi}_k^f$. If we evaluate (16) for $k \in \tilde{t}_j$, the matrices $\tilde{\mathcal{O}}_k^f$, $\tilde{\Phi}_k^f$, and $\tilde{\Psi}_k^f$ are constant. Substituting (15) into (12) and disregarding the effect of the initial state gives

$$\bar{y}_{k+p}^f = \tilde{\mathcal{O}}_j^f (\mathcal{C}_j^p \quad \mathcal{H}_j^p) \begin{pmatrix} \bar{u}_k^p \\ \bar{y}_k^p \end{pmatrix} + \tilde{\Phi}_j^f \bar{u}_{k+p}^f + \tilde{\Psi}_j^f \bar{y}_{k+p}^f + \bar{e}_{k+p}^f \quad \forall k \in \tilde{t}_j \quad (18)$$

An estimate of the matrices $\tilde{\Phi}_j^f$ and $\tilde{\Psi}_j^f$ can be found by performing a linear regression [22, 23] where we assume that the matrix $\tilde{\mathcal{O}}_j^f (\mathcal{C}_j^p \quad \mathcal{H}_j^p)$ has full rank. Subtracting this estimate from (18) we end up with

$$z_{k+p}^j = \bar{y}_{k+p}^f - \hat{\Phi}_j^f \bar{u}_{k+p}^f - \hat{\Psi}_j^f \bar{y}_{k+p}^f \approx \tilde{\mathcal{O}}_j^f x_{k+p} + \bar{e}_{k+p}^f \quad \forall k \in \tilde{t}_j \quad (19)$$

The stacked vectors can be used to build the following matrices

$$\bar{Y}_j^f = (\bar{y}_{i_j,1}^f \quad \bar{y}_{i_j,2}^f \quad \dots \quad \bar{y}_{i_j,x_j}^f), \quad j \in [1, \dots, v] \quad (20)$$

[§]We add to every element of \tilde{t}_j the scalar p .

[¶]Observe that we assume that the matrix \tilde{A} is stable and not A . The rotational dynamics of a wind turbine includes a pure integrator.

where the matrices \bar{U}_j^f and \bar{E}_j^f can be constructed in the similar way, and $\bar{X}_j = x_{\bar{t}_j+p}$. With these definitions, we can write (19) as

$$Z^j = \bar{Y}_j^f - \hat{\Phi}_j^f \bar{U}_j^f - \hat{\Psi}_j^f \bar{Y}_j^f \approx \tilde{\mathcal{O}}_j^f \bar{X}_j + \bar{E}_j^f \quad (21)$$

Equation (21) can be used to determine the observability matrix, $\tilde{\mathcal{O}}_j^f$, and the state sequence, \bar{X}_j , up to a similarity transformation, using the SVD of the matrix Z^j

$$Z^j = (\mathcal{U}_n^j \ \mathcal{U}_{n\perp}^j) \begin{pmatrix} \Sigma_n^j & 0 \\ 0 & \Sigma_0^j \end{pmatrix} \begin{pmatrix} \mathcal{V}_n^{j\top} \\ \mathcal{V}_{n\perp}^{j\top} \end{pmatrix}$$

where Σ_n^j is the diagonal matrices containing n dominant singular values and \mathcal{U}_n^j is the corresponding column space. Note that we can find the dominant singular values by detecting a gap between the singular values. In the limit for $\alpha_j \rightarrow \infty$ and $p \rightarrow \infty$, it then holds that

$$\tilde{\mathcal{O}}_j = \mathcal{U}_n^j T_j \quad (22)$$

$$\bar{X}_j = T_j^{-1} \Sigma_n^j \mathcal{V}_n^j \quad (23)$$

This can be done for all $j = \{1, \dots, v\}$, obtaining different column spaces. The similarity transformations T_j will also be different at each time; hence, the models are identified in a different state basis. With a finite number of data points and past window size still a gap can be detected (see [28] for more detailed information). We have to stress that if the identified states are in the same state basis, the LPV system identification problem is solved.

2.4. Step 2: relating the v -extended observability matrices

For this step we need to relate the different observability matrices to the same basis. This can be done by writing the observability matrices of the different repeating scheduling sequences as a product between a matrix containing only the scheduling terms and a constant matrix that depends only on the system matrices $\tilde{A}^{(i)}$, $C^{(i)}$. This factorization was introduced in [21]. First, define the m -tuple $\mathcal{A} = \{\tilde{A}^{(1)}, \dots, \tilde{A}^{(m)}\}$ containing all matrices $A^{(i)}$ and similarly the m -tuple $\mathcal{C} = \{C^{(1)}, \dots, C^{(m)}\}$ consisting of all matrices $C^{(i)}$. Then define the operator \mathcal{P}_j on these two tuples, which returns the block matrix of all ordered products between one element from \mathcal{C} and $j-1$ elements from \mathcal{A} (m^j possible combinations). Formally, the ζ th block row $\mathcal{P}_j^\zeta(\mathcal{C}, \mathcal{A}) \in \mathbb{R}^{\ell \times n}$ of $\mathcal{P}_j(\mathcal{C}, \mathcal{A}) \in \mathbb{R}^{\ell m^j \times n}$ is given by

$$\mathcal{P}_j^\zeta(\mathcal{C}, \mathcal{A}) = C^{(i_1^\zeta)} A^{(i_2^\zeta)} A^{(i_3^\zeta)} \dots A^{(i_j^\zeta)} \quad (24)$$

with $i_1^\zeta, \dots, i_j^\zeta \in \{1, \dots, m\} \ \forall \zeta \in \{1, \dots, m^j\}$ and ordered by $\rho_{\zeta+1} > \rho_\zeta$ where

$$\rho_\zeta = (i_1^\zeta \ i_2^\zeta \ i_3^\zeta \ \dots \ i_j^\zeta) \begin{pmatrix} m^{j-1} \\ m^{j-2} \\ m^{j-3} \\ \vdots \\ m^0 \end{pmatrix}$$

To illustrate this definition, notice that for $m=2$ one obtains

$$\mathcal{P}_1 = \begin{pmatrix} C^{(1)} \\ C^{(2)} \end{pmatrix}, \quad \mathcal{P}_2 = \begin{pmatrix} C^{(1)} \tilde{A}^{(1)} \\ C^{(1)} \tilde{A}^{(2)} \\ C^{(2)} \tilde{A}^{(1)} \\ C^{(2)} \tilde{A}^{(2)} \end{pmatrix}, \quad \mathcal{P}_3 = \begin{pmatrix} C^{(1)} \tilde{A}^{(1)} \tilde{A}^{(1)} \\ C^{(1)} \tilde{A}^{(1)} \tilde{A}^{(2)} \\ C^{(1)} \tilde{A}^{(2)} \tilde{A}^{(1)} \\ C^{(1)} \tilde{A}^{(2)} \tilde{A}^{(2)} \\ C^{(2)} \tilde{A}^{(1)} \tilde{A}^{(1)} \\ C^{(2)} \tilde{A}^{(1)} \tilde{A}^{(2)} \\ C^{(2)} \tilde{A}^{(2)} \tilde{A}^{(1)} \\ C^{(2)} \tilde{A}^{(2)} \tilde{A}^{(2)} \end{pmatrix}$$

The amount of block rows grows exponentially as m^j . The operator \mathcal{P}_j is used to define

$$S = \begin{pmatrix} \mathcal{P}_1(\mathcal{C}, \mathcal{A}) \\ \mathcal{P}_2(\mathcal{C}, \mathcal{A}) \\ \vdots \\ \mathcal{P}_d(\mathcal{C}, \mathcal{A}) \end{pmatrix} \in \mathbb{R}^{q \times n} \quad (25)$$

Now define

$$M_k^f = \begin{pmatrix} \mu_k^T & 0 & \cdots & 0 \\ 0 & \mu_k^T \otimes \mu_{k+1}^T & \cdots & 0 \\ \vdots & \vdots & \ddots & \vdots \\ 0 & 0 & \cdots & \mu_k^T \otimes \cdots \otimes \mu_{k+f-1}^T \end{pmatrix} \otimes I_\ell \quad (26)$$

with $M_k^f \in \mathbb{R}^{f\ell \times q}$. Then it can be shown by simple substitution and using (9) that

$$\mathcal{O}_j^f = M_j^f S$$

where \mathcal{O}_j^f is known up to an unknown similarity transformation (22), M_j^f depends on the known scheduling sequence (26) belonging to the scheduling sequence j , and S is an unknown matrix defined in (25). Note that the number of rows of S (columns of M_j^f), denoted by q , increases exponentially with f according to the relation $q = \sum_{j=1}^f \ell m^j$. We now give a result that relates the different observability matrices. We present the following result for the noiseless case and for the case that an unbiased estimate has been obtained. Let \mathcal{U}_n^j be equal to \mathcal{O}_j^f up to a similarity transformation such that

$$\mathcal{U}_n^j T_j = \mathcal{O}_j^f$$

Define

$$\begin{aligned}\tilde{\mathcal{U}} &= \text{diag}(\mathcal{U}_n^1, \dots, \mathcal{U}_n^v) \in \mathbb{R}^{dv \times nv} \\ \tilde{\Gamma} &= \text{diag}(\mathcal{O}_1^f, \dots, \mathcal{O}_v^f) \in \mathbb{R}^{fv \times nv}\end{aligned}\quad (27)$$

$$\begin{aligned}\hat{T} &= ((T_1)^T, \dots, (T_v)^T)^T \in \mathbb{R}^{nv \times n} \\ \tilde{M} &= ((M_1^f)^T, \dots, (M_v^f)^T)^T \in \mathbb{R}^{nv \times q}\end{aligned}\quad (28)$$

where M_j^f is defined in (26). Also, define \tilde{T} equal to \hat{T} up to an unknown square invertible matrix $T \in \mathbb{R}^{n \times n}$, now the following relations hold

$$\tilde{T} = \hat{T}T \quad \text{and} \quad \tilde{S} = ST$$

Now we can define

$$\text{null}([\tilde{\mathcal{U}} \quad \tilde{M}]) = \begin{pmatrix} \phi \\ \psi \end{pmatrix}\quad (29)$$

which can also be formulated as an intersection problem. With the condition $\phi \in \mathbb{R}^{nv \times \sigma}$, $\psi \in \mathbb{R}^{q \times \sigma}$, and $\sigma = q + nv - \text{rank}([\tilde{\mathcal{U}} \quad \tilde{M}])$ and $\sigma = n$. Then

$$\begin{aligned}\psi &= ST = \tilde{S} \\ \phi &= \hat{T}T = \tilde{T}\end{aligned}\quad (30)$$

This implies that when the rank conditions hold the matrices S and \hat{T} can be found up to an unknown similarity transformation.

In the case of noise, (29) will lead to a smaller (or even an empty) null space. This can be overcome by using an SVD to compute ϕ and ψ . Furthermore, the dimensions of the intersection problem formulated in (29) grow exponential with the window size f . However, to convert all the states to the same state basis, we only need the similarity transformations. To solve the intersection problem we only require the column space of \tilde{M} . A method for reducing the matrix dimensions is proposed in [21].

2.5. Step 3: recovering of the LPV system matrices

In the previous step, all the states sequences are transformed into the same global state basis. It is well known that when the state, input, output, and scheduling sequences are known the system matrices can be estimated. First we use (2), which is now a linear relation with $C^{(i)}$ and $D^{(i)}$, where e_k represents a white noise. From this equation an estimate can be found for $C^{(i)}$ and $D^{(i)}$ matrices while also the noise sequence can be estimated. The estimated noise sequence is used to transform (1) into a linear expression depending on $A^{(i)}$, $B^{(i)}$, and K . Note that for solving this linear relation, the state should be known at x_k and x_{k+1} and only the data points that have this property are selected. Observe that for periodic systems or almost periodic systems this will always be the case and the complete or almost the complete state sequence is known.

In the example given in Figure 1, the state can be reconstructed at $t_{1,1} + p$, $t_{1,2} + p$, $t_{1,3} + p$, and $t_{1,4} + p$ for $j=1$ with the presented algorithm. For the second constant scheduling segment, $j=2$, the state is estimated at $t_{2,1} + p$, $t_{2,2} + p$, $t_{2,3} + p$, and $t_{2,4} + p$. The second constant segment starts one sample later than the segment belonging to $j=1$. This implies that four linear problems can be formulated where x_{k+1} and x_k are known.

3. SIMULATION STUDY

An LTI system identification is well established and a few applications can be reported in the wind energy [12–15]. However, the techniques used are all based on the open-loop setting and will give biased results in the closed-loop setting [29]. In this paper, we presented an identification approach to identify LPV systems assuming that the scheduling sequence repeats itself a number of times. In this section we use a nonlinear model of the rotational dynamics to illustrate the working of the proposed algorithm. We start this section with the description of the wind turbine model used followed by a simulation to obtain input–output data. In the last part of this section, the simulation results are presented.

3.1. First principle model of a horizontal axis wind turbine

In this paper we consider a seven degrees of freedom model, as described in [4, 30]. The model describes the rotational dynamics of a wind turbine around a particular operating point. The model contains degrees of freedom for the main rotation, first torsion mode of the drive train, the first fore-aft, and sideward bending mode of the tower. In this model, the blades are considered to be rigid. In Figure 2, a schematic representation of the model is given.

Using a linearized conversion of the aerodynamic behavior, the model equations can be given in the following continuous-time LPV system

$$\frac{dx(t)}{dt} = Ax(t) + \left(B^{(0)} + \sum_{i=1}^3 B^{(i)} \varphi^{(i)}(t) \right) u(t) + \left(F^{(0)} + \sum_{i=1}^3 F^{(i)} \varphi^{(i)}(t) \right) v(t) \quad (31)$$

$$y(t) = \left(C^{(0)} + \sum_{i=1}^3 C^{(i)} \varphi^{(i)}(t) \right) x(t) + Du(t) + Gv(t) \quad (32)$$

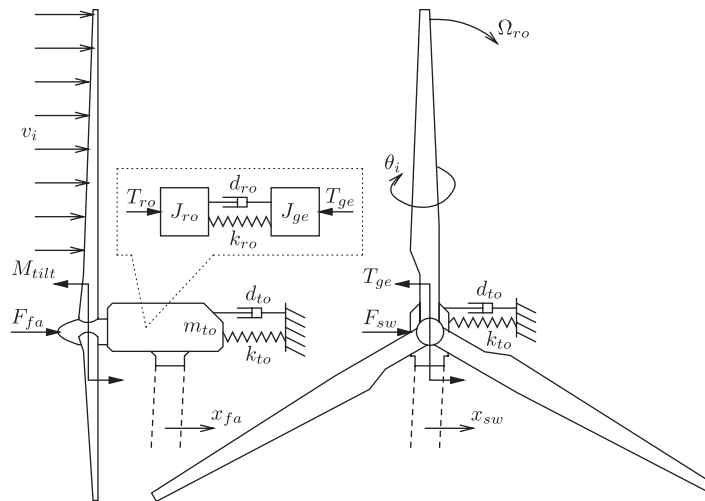


Figure 2. Schematic representation of the wind turbine model.

where the matrices $B^{(i)}$, $C^{(i)}$, and $F^{(i)}$ are multiplied with the scheduling sequence, which is the azimuth angle $\varphi^{(i)}$ of the accompanying rotor blade. The wind turbine model under consideration has three rotor blades ($i = 1, 2, 3$) and is normally used to design IPC controllers. The system state, input, disturbance, and output vector are given by

$$\begin{aligned} x &= (\delta\Omega_{ro} \ x_{fa} \ \dot{x}_{fa} \ x_{sw} \ \dot{x}_{sw} \ \varepsilon \ \dot{\varepsilon})^T \\ u &= (\delta\theta_1 \ \delta\theta_2 \ \delta\theta_3 \ \delta T_{ge})^T \\ v &= (\delta v_1 \ \delta v_2 \ \delta v_3)^T \\ y &= (\delta\Omega_{ge} \ \dot{x}_{fa} \ \dot{x}_{sw} \ \delta M_1 \ \delta M_2 \ \delta M_3)^T \end{aligned}$$

respectively. This model contains thus the control inputs for the variation in generator torque δT_{ge} and the pitch angle $\delta\theta_i$ of each rotor blade. Furthermore, the model contains the inputs for the wind speed disturbance δv_i on each of the three rotor blades. The outputs are the variations in generator speed $\delta\Omega_{ge}$, the fore-aft velocity \dot{x}_{fa} , and the sideward velocity \dot{x}_{sw} of the tower and the blade root bending moment δM_i of each rotor blade. The state contains the variations in rotor speed $\delta\Omega_{ro}$, the fore-aft displacement x_{fa} and velocity \dot{x}_{fa} , the sideward displacement x_{sw} and velocity \dot{x}_{sw} , and the drive-train displacement ε and speed $\dot{\varepsilon}$.

The model under consideration has a constant A matrix, whereas the input and output matrices strongly depend on the azimuth angle, φ . In [4] the Coleman transformation is used to transform this model to an LTI model. The Coleman transformation is a nonlinear transformation that is used to transform the outputs defined in the rotating frame to the fixed nonrotating frame and on a similar way this can be done for the inputs. However, this transformation cannot cope with a failing sensor/actuator, gravity, and yaw misalignment. If the Coleman transformation is applied to these models, still periodic components will be present in the dynamics. However, all the mentioned phenomena will still lead to an LPV model where the system undergoes the same time variation a number of times. Still, in this paper we selected the model given in (31)–(32) based on its simplicity, available documentation [4, 30], and the mentioned phenomena will not change the proposed LPV system identification algorithm.

The constant state-space matrices A , D , and G are given by

$$A = \begin{pmatrix} 0 & 0 & -\frac{3h_{Mx}}{J_{ro}} & 0 & 0 & -\frac{k_{ro}}{J_{ro}} & -\frac{d_{ro}}{J_{ro}} \\ 0 & 0 & 1 & 0 & 0 & 0 & 0 \\ 0 & -\frac{k_{to}}{m_{to}} & \frac{81R}{32H^2} \frac{h_{Mz}}{m_{to}} - \frac{d_{to}}{m_{to}} - \frac{3h_{Fx}}{m_{to}} & 0 & 0 & 0 & 0 \\ 0 & 0 & 0 & 0 & 1 & 0 & 0 \\ 0 & 0 & -\frac{27R}{16H^2} \frac{h_{Fz}}{m_{to}} & -\frac{k_{to}}{m_{to}} & -\frac{d_{to}}{m_{to}} & 0 & 0 \\ 0 & 0 & 0 & 0 & 0 & 0 & 1 \\ 0 & 0 & -\frac{3h_{Mx}}{J_{ro}} & 0 & 0 & -\frac{J_{ro} + J_{ge}}{J_{ro} J_{ge}} k_{ro} & -\frac{J_{ro} + J_{ge}}{J_{ro} J_{ge}} d_{ro} \end{pmatrix} \quad (33)$$

$$D = \begin{pmatrix} 0 & 0 & 0 & 0 \\ 0 & 0 & 0 & 0 \\ 0 & 0 & 0 & 0 \\ k_{Mz} & 0 & 0 & 0 \\ 0 & k_{Mz} & 0 & 0 \\ 0 & 0 & k_{Mz} & 0 \end{pmatrix}, \quad G = \begin{pmatrix} 0 & 0 & 0 \\ 0 & 0 & 0 \\ 0 & 0 & 0 \\ h_{Mz} & 0 & 0 \\ 0 & h_{Mz} & 0 \\ 0 & 0 & h_{Mz} \end{pmatrix} \quad (34)$$

The state-space matrices B , C , and F do have an LPV structure and are given by

$$(B^{(0)} | B^{(i)}) = \left(\begin{array}{cccc|ccc} \frac{k_{Mx}}{J_{ro}} & \frac{k_{Mx}}{J_{ro}} & \frac{k_{Mx}}{J_{ro}} & 0 & & 0 & \\ 0 & 0 & 0 & 0 & & 0 & \\ \frac{k_{Fx}}{m_{to}} & \frac{k_{Fx}}{m_{to}} & \frac{k_{Fx}}{m_{to}} & 0 & & \frac{3}{2H} \frac{k_{Mz}}{m_{to}} & \\ 0 & 0 & 0 & 0 & O_{7 \times (i-1)} & 0 & O_{7 \times (4-i)} \\ 0 & 0 & 0 & \frac{3}{2H} \frac{1}{m_{to}} & & -\frac{k_{Fz}}{m_{to}} & \\ 0 & 0 & 0 & 0 & & 0 & \\ \frac{k_{Mx}}{J_{ro}} & \frac{k_{Mx}}{J_{ro}} & \frac{k_{Mx}}{J_{ro}} & \frac{1}{J_{ge}} & & \underbrace{0}_{\text{ith column}} & \end{array} \right) \quad (35)$$

$$(F^{(0)} | F^{(i)}) = \left(\begin{array}{cccc|ccc} \frac{h_{Mx}}{J_{ro}} & \frac{h_{Mx}}{J_{ro}} & \frac{h_{Mx}}{J_{ro}} & & & 0 & \\ 0 & 0 & 0 & & & 0 & \\ \frac{h_{Fx}}{m_{to}} & \frac{h_{Fx}}{m_{to}} & \frac{h_{Fx}}{m_{to}} & & & \frac{3}{2H} \frac{h_{Mz}}{m_{to}} & \\ 0 & 0 & 0 & O_{7 \times (i-1)} & & 0 & O_{7 \times (3-i)} \\ 0 & 0 & 0 & & & -\frac{h_{Fz}}{m_{to}} & \\ 0 & 0 & 0 & & & 0 & \\ \frac{h_{Mx}}{J_{ro}} & \frac{h_{Mx}}{J_{ro}} & \frac{h_{Mx}}{J_{ro}} & & & \underbrace{0}_{\text{ith column}} & \end{array} \right) \quad (36)$$

$$\left(\begin{array}{c} C^{(0)} \\ C^{(i)} \end{array} \right) = \left(\begin{array}{ccccccc} 1 & 0 & 0 & 0 & 0 & 0 & -1 \\ 0 & 0 & 1 & 0 & 0 & 0 & 0 \\ 0 & 0 & 0 & 0 & 0 & 1 & 0 \\ 0 & 0 & -h_{Mz} & 0 & 0 & 0 & 0 \\ 0 & 0 & -h_{Mz} & 0 & 0 & 0 & 0 \\ 0 & 0 & -h_{Mz} & 0 & 0 & 0 & 0 \\ \hline & & & O_{(i+2) \times 7} & & & \\ 0 & 0 & \frac{9Rh_{Mz}}{8H} & 0 & 0 & 0 & 0 \\ & & & O_{(3-i) \times 7} & & & \end{array} \right) \text{ } (i+3)\text{th row} \quad (37)$$

In these matrices the parameters k_{M_x} , k_{M_z} , k_{F_x} , and k_{F_z} describe the aerodynamic gains from the pitch angle to the root moment, flap moment, root force, and flap force, respectively. The parameters h_{M_x} , h_{M_z} , h_{F_x} , and h_{F_z} describe the gain from the wind speed to the root moment, flap moment, root force, and flap force, respectively. The constants R and H are the rotor radius and the height of the hub, respectively; the mass moment of inertia J , the mass m , the stiffness k , and the damping d . Furthermore, the subscripts ro, to, and ge refer to the rotor, tower, and generator, respectively. The aerodynamic constants are listed in [30] and are derived for a wind speed of 16 m/s, a pitch angle of 10° , and a rotor speed of 1.795 rad/s.

3.2. Simulation of the closed-loop wind turbine model

The LPV system given in (31) and (32) is used to obtain the input, output, and the scheduling sequence for the identification algorithm. For this purpose, the equations are converted to discrete time using a naive zero-order hold discretization method with a sample time of 0.1 s. The naive approach omits the switching behaviors of the sampled scheduling signals. For our case, where the scheduling sequence is a function of the azimuth angles the scheduling sequences are given by the smooth signals

$$\varphi_k = \left(\sin\left(\frac{2\pi k}{v}\right), \sin\left(\frac{2\pi k}{v} + \frac{2\pi}{3}\right), \sin\left(\frac{2\pi k}{v} + \frac{4\pi}{3}\right) \right)^T \quad (38)$$

When an appropriate sample time is chosen, this method gives a good approximation of the continuous time LPV system.

The wind turbine system is not asymptotically stable; it has an integrator, a collective pitch controller in a feedback loop is added to the system to stabilize the system. The controller used can be found in [30] where the collective pitch controller is parameterized. For the pitch-angle inputs, we take an additional zero-mean white noise with $\text{var}(\theta_{k,i}) = 1^\circ$, which is added to the control signal of the collective pitch controller. As input for the generator torque we also take a zero-mean white-noise signal with $\text{var}(T_{ge,k}) = 1 \times 10^6 \text{ Nm}$. The wind disturbance signal is also zero-mean white noise with $\text{var}(v_{k,i}) = 1 \text{ m/s}$, but this signal is assumed to be unknown.

3.3. Closed-loop LPV subspace identification results

The collected data of u_k , y_k , and μ_k from the simulations are used in the identification experiments. The scheduling sequence can be rewritten as $\mu_k = (1 \ \varphi_{k,1} \ \varphi_{k,2})^T$ to fulfill the assumption that this scheduling matrix must be of full rank. The third azimuth angle can be written as a linear combination of the other two angles. For the identification experiments, we used $N = 1000$, $v = 35$, $f = 16$, and $p = 10$.

The performance of the identified system is evaluated by looking at the eigenvalues of the A matrix and the value of the variance accounted for (VAF) on a data set different from the one used for identification. The VAF is defined as $\text{VAF} = \max\{1 - \text{var}(y_k - \hat{y}_k) / \text{var}(y_k), 0\} \times 100$, where \hat{y}_k denotes the output signal obtained by simulating the identified LPV system, y_k is the output signal of the true LPV system, and var is an operator that computes the variance. For meaningful VAF values, the system under consideration must be asymptotically stable, otherwise a small error will give low VAF values due to the increasing or decreasing characteristic of the outputs. This problem occurs for the output of the generator speed; therefore, bode diagrams at a fixed scheduling vector are used to evaluate the performance at those specific channels.

To investigate the sensitivity of the identification algorithm with respect to the wind disturbances, a Monte Carlo simulation with 100 runs was carried out. For each of the 100 simulations, a different realization of the input u_k and wind disturbance v_k is used. In Figure 3, the eigenvalues of the estimated models are compared with the true values. It shows that the identified eigenvalues are very close to the true eigenvalues and that the variance and bias is very small. Figure 4 shows

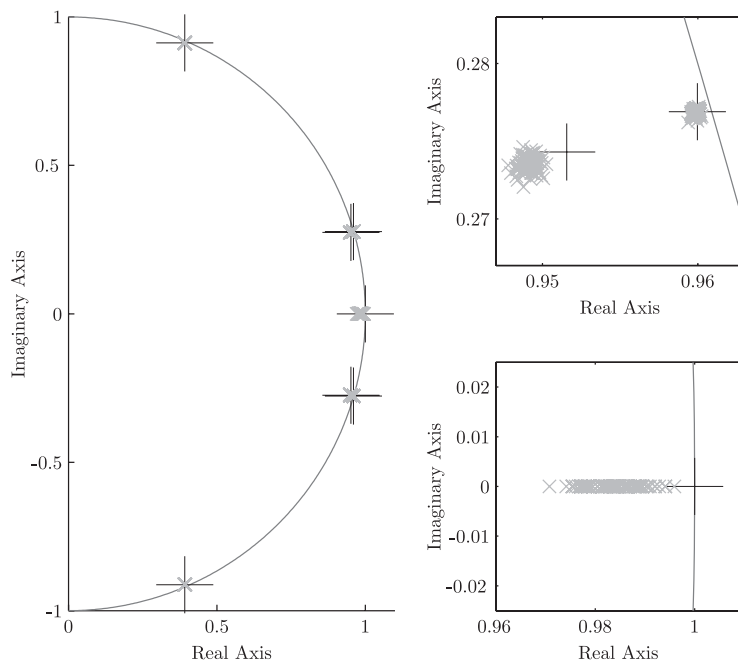


Figure 3. Eigenvalues of the estimated A matrix in the complex plane for 100 experiments with a wind disturbance of $\text{var}(v) = 1 \text{ m/s}$. The big crosses correspond to the real values of the eigenvalues of the matrix. The boxes to the right show a magnification of three pole locations.

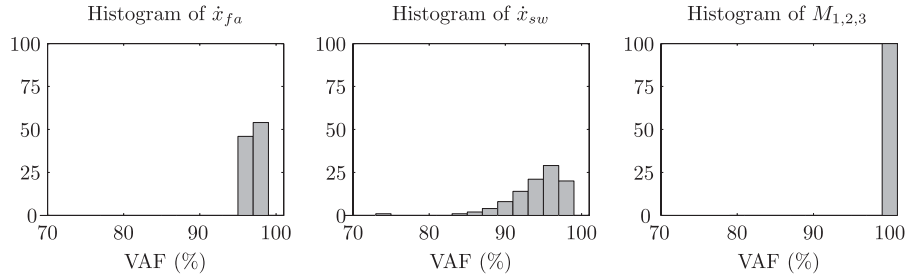


Figure 4. Histogram of VAF values (%) of the outputs \dot{x}_{fa} , \dot{x}_{sw} , and $M_{1,2,3}$. The range of VAF values from 0 to 100% is divided into bins of 2%. For each bin, it is shown how many data sets out of the total 100 resulted in VAF values that fall into that bin.

the corresponding histograms of the VAF values on a fresh validation set with the same scheduling vector and without the wind disturbances. The outputs of the blade root moments M_1 , M_2 , and M_3 score very high VAF values, all within 98 and 100%. The outputs \dot{x}_{fa} and \dot{x}_{sw} are more affected by the wind disturbance. However, the values are still satisfactorily high. The bode diagrams with the generator speed Ω_{ge} as output are given in Figure 5. Also in this figure satisfactory fits are shown, especially for the transfer function with the pitch angles as input. However, for the transfer function between the generator torque and the generator speed, the low frequent behavior shows a large variance due to the high disturbance, which has a significant effect on the estimation of pole belonging to the integrator. However, this is a well-known phenomena in an LTI system identification. The resonance frequency is well estimated and for controller design this resonance frequency will significantly limit the bandwidth.

4. DISCUSSION

For controller synthesis it is important to have accurate mathematical models of the dynamic behavior of wind turbines. However, wind turbines are nonlinear and nonlinear techniques that should be used to synthesize controllers that have guaranteed stability and performance margins over the whole operational range of the turbine. Nonlinear system identification can be used to obtain accurate models for controller synthesis. In this paper we showed an LPV system identification scheme to identify the rotational dynamics of a horizontal axis wind turbine (HAWT). However, we assumed to have a dedicated scheduling sequence. That is a valid assumption for the simulation example but the dynamics of the wind turbine is also strongly dependent on the wind speed and this quantity cannot be made periodic. The big challenge from an identification point of view for the wind energy is to develop efficient algorithms to deal with LPV systems with random scheduling.

5. CONCLUSION

Wind turbines are nonlinear systems, although their nonlinearity is linearly dependent on measurable scheduling signals and therefore they can be modeled in the LPV framework. With LPV controller synthesis, which is strongly related to robust controller design, gain-scheduled controllers can be calculated with guaranteed stability and performance margins. In this paper we discussed

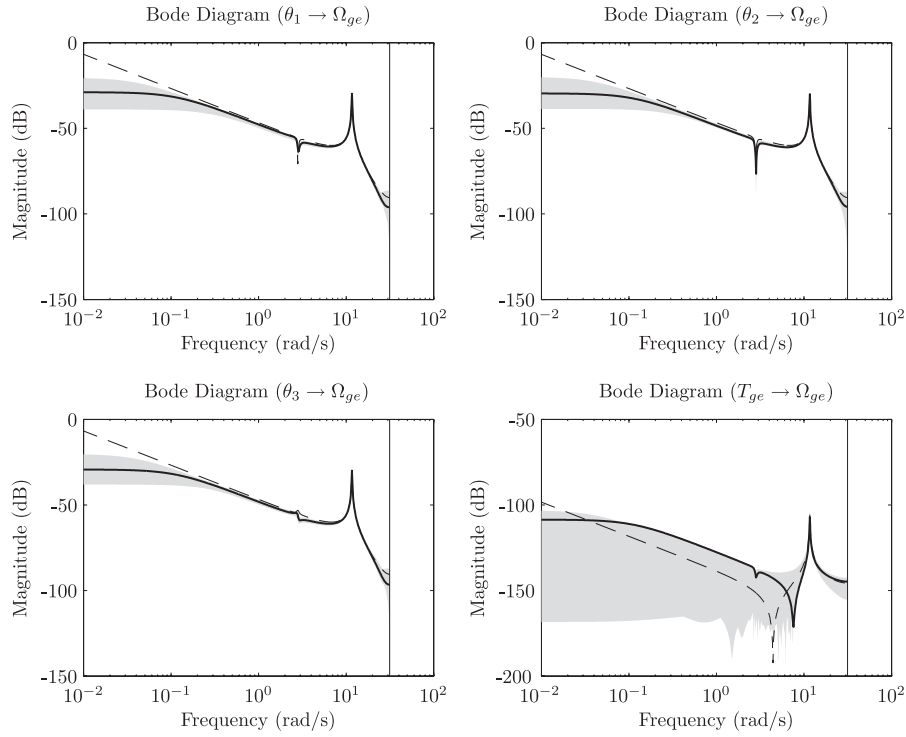


Figure 5. Bode diagrams of the original transfer functions (dashed) and the identified transfer functions of the experiment with the highest mean VAF value (bold). The transfer functions of the other 99 experiments are within the gray confidence region. To determine the bode diagram, the azimuth angles are fixed at the values $\varphi = (0, \sqrt{3}/2, -\sqrt{3}/2)$.

LPV system identification and we proposed a subspace algorithm to identify the rotational dynamics of a HAWT. We exploited the fact that the system experienced the same time variation a number of times. We used LTI system identification techniques to identify a number of observability matrices and state sequences that are, inherent to subspace identification, identified in a different state basis. We showed that by formulating an intersection problem all the states can be reconstructed in a general state basis from which the system matrices could be estimated. We showed the working of the proposed algorithm on a nonlinear model of a wind turbine that was operating in closed loop.

ACKNOWLEDGEMENTS

This research is supported by the Technology Foundation STW, applied science division of NWO, and the technology program of the Ministry of Economic Affairs.

REFERENCES

1. Manwell JF, McGowan JG, Rogers AL. *Wind Energy Explained; Theory, Design and Application*. Wiley: Chichester, 2002.
2. Bossanyi EA. The design of closed loop controllers for wind turbines. *Wind Energy* 2000; **3**:149–163.

3. Bossanyi EA. Further load reductions with individual pitch control. *Wind Energy* 2005; **8**:481–485.
4. Engelen TG. Design model and load reduction assessment for multi-rotational mode individual pitch control. *European Wind Energy Conference (EWEC2006)*, Athens, Greece, 2006.
5. Larsen TJ, Madsen HA, Thomsen K. Active load reduction using individual pitch, based on local blade flow measurements. *Wind Energy* 2005; **8**:67–80.
6. Hand MM, Balas MJ. Blade load mitigation control design for a wind turbine operating in the path of vortices. *Wind Energy* 2007; **10**:339–355.
7. Shamma J, Athens M. Guaranteed properties of gain scheduled control for linear parameter varying plants. *Automatica* 1991; **27**:559–564.
8. Bianchi FD, Mantz RJ, Christiansen CF. Control of variable-speed wind turbines by LPV gain scheduling. *Wind Energy* 2004; **7**:1–8.
9. Bianchi FD, Mantz RJ, Christiansen CF. Gain scheduling control of variable-speed wind energy conversion systems using quasi-LPV models. *Control Engineering Practice* 2005; **13**:247–255.
10. Lescher F, Zhao JY, Martinez A. Multiobjective H_2/H_∞ control of a pitch regulated wind turbine for mechanical load reduction. *European Wind Energy Conference*, Athens, Greece, 2006.
11. Molenaar D-P. Cost effective design and operation of variable speed wind turbines. *Ph.D. Thesis*, Technical University of Delft, 2003.
12. van Baars GE, Mosterd H, Bongers PMM. Extension to standard system identification of detailed dynamics of a flexible wind turbine. *Proceedings of the 32nd Conference on Decision and Control*, San Antonio, TX, 1993; 3514–3519.
13. Hansen MH, Thomsen K, Fuglsang P, Knudsen T. Two methods for estimating aeroelastic damping of operational wind turbine modes from experiments. *Wind Energy* 2006; **9**:179–191.
14. James III GH, Carne TG, Lauffer JP. The natural excitation technique (NExt) for modal parameter extraction from operating wind turbines. *Technical Report*, Sandia, 1993.
15. Knudsen T, Andersen P, Toffner-Clausen S. Comparing PI and robust pitch controller on a 400 kW wind turbine by full scale tests. *Proceedings of the European Wind Energy Conference*, Dublin, 1997.
16. Verdult V. Nonlinear system identification: a state space approach. *Ph.D. Thesis*, University of Twente, 2002.
17. Verdult V, Verhaegen M. Subspace identification of multivariable linear parameter-varying systems. *Automatica* 2002; **38**(5):805–814.
18. Verdult V, Verhaegen M. Kernel methods for subspace identification of multivariable LPV and bilinear systems. *Automatica* 2005; **41**:1557–1565.
19. Verdult V, Bergboer N, Verhaegen M. Identification of fully parameterized linear and nonlinear state-space systems by projected gradient search. *The IFAC Symposium on System Identification (SYSID)*, Rotterdam, 2003; preprint.
20. van Wingerden JW, Felici F, Verhaegen M. Subspace identification of MIMO LPV systems using piecewise constant scheduling sequence with hard/soft switching. *Proceedings of the European Control Conference*, Kos, 2007.
21. Felici F, van Wingerden JW, Verhaegen M. Subspace identification of MIMO LPV systems using a periodic scheduling sequence. *Automatica* 2007; **43**(10):1684–1697.
22. Chiuso A, Picci G. Consistency analysis of certain closed-loop subspace identification methods. *Automatica* 2005; **41**:377–391.
23. Chiuso A. The role of vector auto regressive modeling in predictor based subspace identification. *Automatica* 2007; **43**(6):1034–1048.
24. Jansson M. A new subspace identification method for open and closed loop data. *Sixteenth IFAC World Congress*, Prague, Czech Republic, 2005.
25. Rugh WJ. *Linear System Theory*. Upper Saddle River, 1996.
26. Verhaegen M, Yu X. A class of subspace model identification algorithms to identify periodically and arbitrarily time varying systems. *Automatica* 1995; **31**(2):201–216.
27. Knudsen T. Consistency analysis of subspace identification methods based on a linear regression approach. *Automatica* 2001; **37**:81–89.
28. Bauer D. Order estimation for subspace methods. *Automatica* 2001; **37**:1561–1573.
29. van den Hof PMJ, Schrama RJP. Identification and control—closed-loop issues. *Automatica* 1995; **31**:1751–1770.
30. van Engelen T, Markou H, Buhl T, Marrant B. Morphological study of aeroelastic control concepts for wind turbines. *Technical Report*, Energy Research Center (ECN), 2007.